HHS Public Access

Author manuscript

Neuron. Author manuscript; available in PMC 2015 April 09.

Published in final edited form as:

Neuron. 2008 February 28; 57(4): 599–613. doi:10.1016/j.neuron.2007.12.024.

Embodied Information Processing: Vibrissa Mechanics and Texture Features Shape Micro-Motions in Actively Sensing Rats

Jason T. Ritt, **Mark L. Andermann**, and **Christopher I. Moore**

Abstract

Peripheral sensory organs provide the first transformation of sensory information, and understanding how their physical embodiment shapes transduction is central to understanding perception. We report the first characterization of surface transduction during active sensing in the rodent vibrissa sensory system, a widely used model. Employing high-speed videography, we tracked vibrissae while rats sampled rough and smooth textures. Variation in vibrissa length predicted motion mean frequencies, including for the highest velocity events, indicating that biomechanics, such as vibrissa resonance, shape signals most likely to drive neural activity. Rough surface contact generated large amplitude, high velocity “stick-slip-ring” events, while smooth surfaces generated smaller and more regular stick-slip oscillations. Both surfaces produced velocities exceeding those applied in reduced preparations, indicating active sensation of surfaces generates more robust drive than previously predicted. These findings demonstrate a key role for embodiment in vibrissal sensing, and the importance of input transformations in sensory representation.

INTRODUCTION

In all sensory systems, perception and sensory neural activity require peripheral transduction. Information reaching central areas can depend crucially on embodiment, as a sensor’s intrinsic biomechanical properties will shape the energy that is extracted from the environment and translated into neural activity. For example, the range of sound waves a listener perceives is limited in large part by the frequencies the cochlea can detect, and the spatial map of frequencies found in the cochlea lays the foundation for central neural maps of sound frequency [1]. Understanding transduction of sound by the cochlea, and more specifically how its biomechanical properties shape signal transmission, has been crucial to advancing our knowledge of auditory perception [1, 2].

The rat vibrissa sensory system is a popular choice for studies of mammalian sensory processing, in large part because of the regular columnar architecture present in primary somatosensory cortex, the “barrel” columns [3, 4]. This system is also ideal for studying the consequences of sensor embodiment, as the vibrissae are exteriorized thin, stiff hairs with afferents localized to follicles at the base, discretely separating the mechanical and neural

phases of transduction. However, despite the importance of this model system and the extensive characterization of its neural response properties in anesthetized animals, relatively little is known about the transduction of information by the vibrissae during the active sensation of a surface. Indirect evidence from neurophysiological [5–9], behavioral [10–12] and biomechanical studies [9, 13, 14] suggest that small amplitude, high velocity and high frequency events are an essential perceptual cue. As first suggested by Carvell and Simons [11], vibrissa interactions with these surfaces are likely to generate “micro-motions”, up to the thousands of Hertz, that are believed to support the high acuity rats have for texture discrimination [10, 12]. Direct measurement of the neural correlates of surface discrimination in behaving rats is inconclusive, with one study finding no difference in SI multi-unit firing rates between rough and smooth contact [15], but a more recent study finding a small increase in multi-unit activity during rough contact, that correlated with the animal’s decision [16]. These studies determined only epochs of surface contact, without measuring the vibrissa micro-motions that would have served as inputs to the system during the task. Research has proceeded without a thorough understanding of these signals because the inherent challenges in tracking high-speed, small-amplitude motion of thin vibrissae in a freely behaving animal precluded direct measurement of micro-motions.

A principal debate over the character of micro-motions concerns the potential contribution of intrinsic vibrissa mechanics. Of particular interest is the possibility that differences in vibrissa properties across the face result in parallel afferent pathways carrying different information [13, 17–21]. In anesthetized rats and when plucked, vibrissae can act as under-damped elastic beams, demonstrating high-frequency resonant oscillations and substantial (10-fold) amplification of oscillatory stimuli at appropriate frequencies [6, 13, 18, 19] (see also [19] for an example of oscillation in an awake animal). In line with this mechanical model, a vibrissa’s length predicts its resonance frequency, with longer vibrissae expressing lower tuning [13, 19]. Further, the stereotyped organization of lengths across the mystacial pad (shorter anterior hairs) results in a rostral-caudal gradient of frequency along the face [13] that in anesthetized animals induces a frequency column map in primary somatosensory cortex [6]. These observations in reduced preparations led to the hypothesis that resonant phenomenon impact signal transduction in awake behaving animals.

However, other studies in anesthetized *in vivo* and *ex vivo* conditions have argued against this hypothesis, concluding that intrinsic mechanics do not play a significant role in contact-induced micro-motions [9, 14, 21]. Central to the proper interpretation of these conflicting results is the accuracy of their simulation of an animal’s active sensing strategy. The most notable sensing behaviors during exploration are ‘whisking,’ the rhythmic movement of the vibrissae repeatedly against and over objects [10, 22, 23], and head motions [10, 24, 25]. Although informative, previous micro-motion studies used simulated whisking that may deviate from behavioral ground truth [9, 11, 13, 14, 26]. A variety of active sensing choices - including vibrissa sweep speed, tension in the follicle, and which vibrissae contact a surface - could alter the resulting contact-induced micro-motions [18]. Understanding the signals processed in this key model system, and resolving debates about the role of intrinsic vibrissa mechanics, requires overcoming the difficulties in measuring such motions in behaving animals.

In the present study, we describe the first observations of vibrissa micro-motions generated during free behavior, recorded using high-speed (~3.2 kHz) and high-resolution (~100μm) videography and automated vibrissa tracking. We recorded small amplitude, high velocity and high frequency micro-motions of vibrissae as freely behaving rats sampled rough and smooth textured surfaces (complemented by additional *ex vivo* recordings using similar techniques). The goals of the current study were threefold: First, to determine the range of natural vibrissa micro-motions in freely behaving animals interacting with textured surfaces; second, to test the hypothesis that intrinsic mechanics significantly impact vibrissa motions during free behavior; and third, to examine differences in transduction with surface type, for possible cues used by an animal during surface discrimination.

We found that the range of micro-motion velocities and amplitudes substantially exceeds previously utilized stimulation paradigms, suggesting that natural surface engagement produces a significantly stronger input signal than previously appreciated. We further observed that resonant phenomena, as demonstrated in previous mechanical and neural studies [6, 13, 19], shape the frequency of micro-motions during free behavior. We also found and characterized systematic differences in the distribution of events as a function of surface type. These findings provide the first information about micro-motion signals in this key model system, and provide a quantitative context for future probes of this system in reduced preparations. We conclude that under sensing strategies chosen by freely behaving animals, intrinsic mechanics alter sensory transduction such that vibrissae should not be considered as interchangeable, signal-neutral sensors.

RESULTS

Potential Impact of Embodiment and ‘Sampling Strategy’ on Input Signals

Alteration of Resonance Expression with Sampling Strategy—To provide a framework for understanding how natural, active sensing choices can shape signal transduction in vibrissae, we first present *ex vivo* measurements. Elasticity is a key way that the intrinsic filtering properties of vibrissae may impact signal transduction. A principal consequence of vibrissa elasticity is resonance, the selective amplification of a specific range of frequencies in a driving stimulus. Resonance has been demonstrated during *ex vivo* application of sinusoidal input through a stimulator clamped to the vibrissa tip, when a drum covered in sandpaper was rolled tangential to a vibrissa, and in limited *in vivo* contexts, such as the oscillation of a vibrissa in air after springing past contact with a bar [6, 13, 19]. These studies fixed the base and applied a range of stimuli to the tip [6, 13]. In contrast, recent acute studies concluding resonance is not significant attempted a more realistic simulation of whisking behaviors by actuating the vibrissa base such that the tip ran over a fixed surface [9, 14]. However, these studies did not explore different sensing behaviors, in particular by varying sweep speed. Thus the extent to which the divergent results can be attributed to the methods of stimulus delivery and/or the choice of sampling parameters remains unclear.

We attached single vibrissae to a computer-controlled torque motor (see **Methods**, Figure 1A) and swept them against surfaces while varying speed, distance and surface type. Figure 1B shows the micro-motion velocities generated by sweeping a C3 vibrissa over a periodic grating at speeds comparable to free whisking behavior [10]. For the lower (450°/sec) and

higher (810°/sec) sweep speeds, relatively small oscillatory micro-motions were generated by vibrissa-surface interactions. In contrast, at a sweep speed of 630°/sec, large amplitude oscillations developed over the first 60 msec of contact. This selective amplification of surface features likely reflects a match between the spatial frequency of the grating, the resulting temporal frequency generated by contact at a given sweep speed, and the fundamental resonance frequency of the vibrissa (given the distance to the surface and spacing of the grating, the approximate stimulation rates were 150, 210 and 270 Hz for the three sweep speeds). The grating was similar in spatial period (1.28 mm spacing) to 'rough' textures previously employed [10, 11] to test rat psychophysical acuity for textural properties. These 'artificial whisk' speeds overlap the sweep speeds chosen by behaving animals in those studies, and measured at higher resolution recently in a different task context [27]. Further, response amplification was observed within a duration of surface contact (60 msec) that is realistic for vibrissa interactions with a textured surface, as shown in the behavioral data described below, and as inferred from the typical period of a whisk motion over texture [10, 11] (see also [9]).

The dependence of resonance expression on sweep velocity shown in Figure 1B can be understood by the general framework schematized in Figure 1C that describes the separate contributions of surface features, intrinsic mechanics, and active sensing choice in producing micro-motions. In this representation, sweep speed is on the x-axis, and response frequency along the y-axis. There are three key features of this schema. First, a horizontal band indicates resonant frequency tuning. The band is horizontal as resonance frequency is an intrinsic physical property of the vibrissa (for fixed boundary conditions) independent of sweep speed. Second, diagonal bands indicate the temporal frequencies induced by sweeping over surface features with a fixed spatial period. These bands have a predetermined slope; for example, doubling the sweep speed must double the temporal frequency induced by the surface. Third, a gold "sweet spot" indicates the selective amplification of a surface feature driven oscillation at the sweep speed that puts it within the resonance tuning band. The importance of this model lies in its explanation that expression of intrinsic filtering is essentially dependent on active sensing choices under the animal's control, in this case sweep velocity (see Figure 7 of [13] for demonstrations of these components in *ex vivo* examples). Without varying sweep speed, it could be difficult to decompose vibrissa responses into components due to surface features and components due to intrinsic mechanics. With regards specifically to the failure to see the signature of resonance in previous studies, actuation from the base does not itself impair resonance expression, and the lack of variation in sweep speed in previous studies can explain the interpretation that resonance did not occur.

Alteration of Time Domain Patterns with Sampling Strategy—In the above example we described the micro-motion frequency response, and how it can be impacted by active sensing choices. On a finer timescale, significant variation can exist in the specific micro-motion patterns that constitute the response. These temporal patterns are also shaped by active sensing choices available to behaving animals.

Figure 1D (*top*) shows a timeseries of micro-motions for a C3 vibrissa (length 22.5mm) during contact with 80-grit sandpaper. Reliable patterns of micro-motions were observed,

with small variance across 8 trial repetitions within each condition (overlaid in each plot). Similar response consistency held for sweeps over a periodic grating (1.28mm) and glass, and in two additional vibrissae tested across a similar set of conditions (data not shown). This response consistency agrees with that found in previous *ex vivo* and anesthetized studies [9, 14].

Based on the stereotypy of these responses, one might conclude that the micro-motions are due entirely to transduction of the surface profile, as previously argued [9, 14]. However, varying sweep speed can introduce marked changes in micro-motion response (Figure 1D, *bottom*), showing that inputs cannot be considered to be a veridical transmission of surface profile, and that intrinsic elastic properties may shape acquired information. When the sweep speed is increased from 540 to 720°/sec, with all other parameters (including points of contact with the surface) kept constant, the profile of micro-motions differed substantially, with much larger amplitude and irregular deviations observed at the faster sweep. However, the within-condition variance remained small, showing that this alteration of micro-motion pattern was not simply an increase in noise, or other non-specific change. This example demonstrates two transmission modes --- one characterized by smaller and more regular oscillatory motions, and one characterized by less periodic and more ballistic events ---whose relative expression depends on sampling strategy. Both kinds of event patterns were observed in data from actively sensing animals, as described below.

In summary, the *ex vivo* examples emphasize that a given micro-motion or pattern of micro-motions is neither “intrinsic” nor “extrinsic”. Rather, surface properties are filtered through the intrinsic mechanics as a function of active sensing choices.

Signal Transduction During Active Sensation By Behaving Animals

Active Sensing Behaviors During Surface Contact—To examine micro-motions generated during active sensing, we trained rats to perform a forced choice discrimination task that engaged sustained vibrissa contact with rough and smooth surfaces (see **Methods**). Figure 2A shows a schematic of the behavior apparatus. On each trial, removal of a door allowed rats to traverse a short platform to approach the discriminandum, consisting of a rough and a smooth texture to either side of the midline. Each rat was trained to approach a left or right reward port corresponding to the target surface (e.g. always go to the side with the smooth texture). Our focus in this study was to characterize micro-motions generated during active sensing, and we selected surfaces widely divergent in roughness, providing a range in surface impacts on micro-motions. A broad contrast in rough and smooth texture also was chosen to be an “easy” discrimination (compared to previously reported similar tasks [10, 11]) that would recruit regular vibrissa contact. Rats achieved high performance following training (see Supplemental Data S1 for sample behavioral curves and for controls for visual and olfactory cues; see also **Discussion**).

Rats showed stereotyped patterns of surface exploration, as illustrated in Supplemental Movies S2 and S3. Rats approached the surface while whisking their vibrissae forward, and made sustained contact with several vibrissae of different lengths, primarily anterior to and including the 2nd arc. As a typical example, Figure 2 presents vibrissa lengths and contact probabilities in a single session (N=20 vibrissae, 4 high speed videos; see Supplemental

Data S1). Figure 2B shows vibrissa lengths as a function of arc position, demonstrating the anterior-posterior gradient in agreement with previous reports [13, 17, 19]. Figure 2C shows the probability of vibrissa contact as a function of arc position for the initial approach of the animal, up to the putative decision point where a head turn was made towards a reward port. We analyzed the 20 vibrissae (A through D rows and the greek arc through the 4th arc) that were visible and within acceptable focus in each of the videos. In this initial approach phase, more posterior vibrissae (greek and 1 arc) almost never contacted the surface, while the 2–4 arcs regularly did so, with probability of contact >0.55 for any given vibrissa in these arcs. In every video, at least one vibrissa from each of the 2, 3, and 4 arcs contacted the surface, while contact by the 1 arc vibrissae was never unequivocally observed. This contact was typically sustained for the 3 and 4 arcs, while more posterior arcs 'tapped' the surface [10, 11, 25, 28]. During movement to the port, rats subsequently contacted the surface with vibrissae throughout the pad including the more posterior arcs, and sustained this contact until reaching the reward port. The distance of the rat face from the surface was consistent following initial contact and during the subsequent head sweep, ~5 mm from the surface.

Phenomenology of Vibrissa Micro-Motions During Active Sensation of a Rough Surface—Four key features typified micro-motions generated when rats contacted a rough surface with their vibrissae. First, there were distinct periods where the point of vibrissa contact was 'stuck,' and did not move forward, despite forward motion at the vibrissa base due to head motion or vibrissa pad contraction. Second, epochs of sticking against the surface were followed by ballistic, high velocity vibrissa motions ('slips'). Third, distinct periods of high frequency oscillation were observed, often after a sharp deceleration caused by re-sticking, leading to a 'ringing' motion of the vibrissa. Fourth, high frequency motions could mix rhythmic and aperiodic characteristics in irregular 'skipping' motions over the surface. Each of these features can be appreciated in the traces shown in Figure 3, sampled from three distinct vibrissae that were simultaneously in contact with the surface. This behavior is also evident in the Supplemental Movies (see also Figure 7, below). This pattern suggests that during contact with the rough surface, vibrissae exhibited spring-like loading, of the type that routinely engaged pronounced elastic behavior in our *ex vivo* data, and that led to ballistic, high velocity, and large amplitude surface interactions shown in Figure 1D.

Length Determined Frequency Tuning Under Free Behavior—If the intrinsic properties of the vibrissae shape sensory transmission during active sensing, a central prediction is that vibrissa length should influence micro-motion frequency, with higher frequencies in smaller vibrissae [13, 18, 19, 29]. Figure 4A shows micro-motions for two vibrissae of different lengths originating from the same side of the face, during simultaneous interaction with the rough surface. For this we tracked vibrissae near the contact point (see **Methods**), as fundamental resonance frequency estimates should be largely independent of the point tracked, and we obtained multi-whisker micro-motion distributions without having to track the full length of the vibrissa to the base. Distinct patterns of intermittent oscillatory behavior were evident in motions of each of these vibrissae. To analyze the frequency characteristics of these signals during surface contact, we performed a Hilbert transform on the vibrissa motion (shown in grayscale in Figure 4A). This approach, as opposed to a

standard Fourier transform, facilitated characterization of the frequency distribution of the often intermittent (non-stationary) micro-motion epochs. As shown in Figure 4B, the distinct oscillations evident in these two vibrissae were reflected in the distribution of frequencies expressed, with the longer vibrissa (25.5 mm) displaying a mean transduction frequency of 63.6 Hz ± 30.5 SD, and the shorter vibrissa (11.1 mm) a mean frequency of 132.9 Hz ± 58.0 SD. The transmission of distinct mean frequencies was observed across all vibrissae measured on this trial (N = 5), with distinct peaks in transmission in the range between ~50 and ~150 Hz (Figure 3B).

When all tracked vibrissae were included, frequency maintained a linear relationship with vibrissa length ($1/L^2$) (N = 19 vibrissae, 2 rats, 3 trials, minimal contact duration of 44 msec against the rough surface). The $1/L^2$ relationship is expected from mechanical principles [13, 19, 29]. Figure 4C shows the systematic dependence on length ($r^2 = .57$; $p < .001$; slope = 4.63×10^3 Hz*mm^2). This relation held across the broader sample of vibrissae, and within individual trials with multi-vibrissa contact (see examples in Figure 4A–B and symbols within Figure 4C).

Phenomenology of Smooth Surface Contact: Smaller-Amplitude Oscillatory Motions—Oscillatory micro-motions were also observed during vibrissa contact with a smooth surface, suggesting the presence of frictional interactions even in the absence of macroscopic textural features. This behavior also occurred *ex vivo* during sweeps over glass (Figure 5A) in contrast to other *ex vivo* reports [9, 14]. Figure 5B and the top trace in Figure 5C show examples in the behaving animal.

Compared to sweeps over the rough surface, smooth surface interactions exhibited more epochs of periodic skip motions, without epochs of irregular sticking followed by ringing. These oscillatory vibrissa motions were typically smaller than those generated during rough surface contact, and only a subset of vibrissae demonstrated measurable oscillations in this condition. This variability can be seen by comparing traces from two simultaneously tracked vibrissae in Figure 5C. While the upper trace displays clear periods of large amplitude periodic behavior, the bottom trace does not show oscillations. Of the 22 vibrissae quantitatively analyzed, 7 failed to demonstrate residual motions greater than 100μm at the tip. When oscillatory behavior was observed during smooth contact, these micro-motions demonstrated a significant linear relation between the frequency of signal transduction and vibrissa length ($1/L^2$), as shown in Figure 5C (N = 15 vibrissae, 2 rats, 4 trials; $r^2 = .68$; $p < .001$; slope, 9.88×10^3 Hz*mm^2).

Resonance Impacts the Expression of the Highest Velocity Micro-Motions—An important question posed by the analysis described in Figures 4 and 5 is whether the correlation between length and frequency has a significant impact on ‘important’ transduction events. Specifically, does this relationship emerge from the analysis of a large number of low velocity micro-motions, or does it shape high-velocity motions that are believed to have the largest impact on neural firing [5, 7]? To address this question, we restricted this analysis to the highest 10% velocity micro-motions in each timeseries.

Figure 6A shows a trace of vibrissa motion in which the time points of highest velocities are demarcated in red. Plotting the mean frequencies expressed during the highest velocity epochs against vibrissa length showed the same relationship as for the entire timeseries (Figure 6B). Specifically, a significant linear relationship was observed for rough and smooth surface contact (rough (red squares): N = 19 vibrissae, 2 rats, 3 trials; $r^2 = .45$; $p < .01$; slope, 4.63 $x10^3$ Hz*mm^2; smooth (blue circles): N = 15 vibrissae, 2 rats, 4 trials; $r^2 = .73$; $p < .001$; slope, 8.94 $x10^3$ Hz*mm^2). These data show that resonance was not the product of 'background' oscillations, but directly shaped the highest velocity, and putatively most relevant, micro-motions.

Velocities, Amplitudes and Rise Time of Events During Active Sensing—To measure the absolute velocities, amplitudes and rise times of micro-motion events, we tracked the full length of vibrissae in head-centered coordinates (see **Methods**). We report velocities 5mm from the face, as an estimate of signals delivered to follicle afferents, and to provide a comparison to typical stimulus delivery in anesthetized physiology studies [5, 30]. An 'event' was defined as a shift in the angle of the vibrissa relative to its path due to head and whisking motions. In most neurophysiological studies in anesthetized or immobilized animals, a vibrissa is moved from a stationary position, creating a fast angular deflection away from and then returning to 'rest'. In the present context, the effects of head motion and whisking were excluded from the data through tracking of the face and using a 2-band spline fitting method that removed lower-frequency components of the signal but left higher-frequency micro-motions intact (see **Methods** and Supplemental Data S1). Figure 7A shows example timeseries of vibrissa angular velocities in head centered coordinates, with the fits used to measure events overlaid for comparison. Inspection of these timeseries illustrates key trends in the data. First, epochs of regular oscillatory surface interactions were more common during smooth surface interactions (blue background), but were also present in epochs of rough surface contact (red background). Second, independent of regularity, the traces show the general trend from lower to higher frequency vibrations with shorter vibrissae (top to bottom). Third, a number of conjointly large amplitude and high velocity events were observed during rough surface contact.

Observed micro-motion events during active surface palpation showed broad distributions of velocities, amplitudes and rise times (Figure 7B; N = 250 events; N = 11 tracked vibrissae, 8 epochs of rough contact, 6 epochs of smooth contact, 3 vibrissae measured during contact with both; mean duration of contact, 76 msec ± 31 SD). The mean and median amplitude across all events were 0.98° ± 1.66 SD and 0.51°, respectively, the rise time mean and median were 1.42 msec ± 1.84 SD and 0.89 msec, and the velocity mean and median were 1612°/sec ± 1589 SD and 1125°/sec. For velocity and rise time, the means did not differ significantly between rough and smooth contact (mean velocities, rough: 1653°/sec + 1728, smooth: 1566°/sec ± 1417, one-way ANOVA $p>0.6$; mean rise times, rough: 1.48msec ± 1.54 SD, smooth: 1.35msec ± 2.12 SD, one-way ANOVA $p>0.5$;). The mean amplitude was significantly greater on rough than smooth contact (mean amplitudes, rough: 1.20° ± 2.13 SD, smooth: 0.73° ± 0.80 SD, one-way ANOVA $p<0.01$).

The joint distribution across peak velocity and rise time reveals more clearly this separation between events generated by rough versus smooth contact. Figure 8A shows a scatterplot of

all events for peak velocity and the rise time. The means (solid line) and medians (dashed line) of velocity and rise time are indicated. Rough surface contact generated a distinct class of large amplitude (long rise time and high velocity) events. For those events that jointly exceeded the mean velocity and rise time, 80% (12 of 15) were observed during contact with the rough surface. The mean amplitude of events in this group was 5.46° ± 5.27 SD, ~5 times the population mean. Similarly, for events jointly exceeding the median velocity and rise time, 73% (51 of 70) were observed during contact with the rough surface. This group had an average amplitude of 2.59° ± 2.97 SD, ~2.5 times the population mean.

These large amplitude events are expected from the traces of motion over rough stimuli (Figures 3, 4 and 7). During rough contact, a vibrissa could be stuck for a sustained period while the face moved laterally, creating a long duration event, and then would spring forward in a large amplitude, high velocity lunge. This kind of surface interaction was not observed during smooth surface contact. As indicated in the above description of smooth surface interactions, oscillatory skipping of vibrissae over the surface was more common, generating a larger number of smaller amplitude motions.

Observed Micro-Motions Extend Beyond the Range Assessed in Previous Studies of Physiology and Psychophysics—Results in previous acute studies suggest that a significant fraction of micro-motions in freely behaving rats should drive peripheral and cortical neural activity, and moreover should be perceptually superthreshold. Figure 8B plots stimulus ranges employed in previous anesthetized studies of neural responses over the motions we observed during natural surface exploration. For example, in parametric studies (e.g. [5, 31–33]), Simons and colleagues tested peak velocities up to ~2500°/sec, and motion amplitudes up to ~8°, and found that throughout this range the velocity, and not the amplitude, of vibrissa motion predicted the magnitude of cortical responses (Figure 5B, blue region). This full range evoked action potential responses in the periphery and thalamus [5, 31–33]. Diamond and colleagues [7] employed frequencies from 19 Hz to 341 Hz and, by varying the amplitude of these oscillations, generated peak velocities from ~5°/sec to ~1700°/sec (Figure 5B, green region). They similarly found that neural responses in barrel cortex were most sensitive to the velocity of motion (see also [9]). Deschenes and colleagues [34] utilized stimuli encompassing the ranges of the above studies, and although they did not report systematic measurements of response magnitude with changes in amplitude and frequency, they found brainstem and in some cases thalamic responses could precisely follow high frequency inputs (~200 Hz). Contreras and colleagues employed somewhat higher amplitude stimuli, but with peak velocities (1300°/sec) below the mean peak velocity observed during active sensation, that drove sub- and suprathreshold cortical responses [35, 36] (Figure 5B, black curve with triangles marking stimulus values). Andermann and Moore (2006) employed a mean angular deviation (1.3°) slightly above that observed during active sensing of rough texture, and found that velocities several-fold smaller (260°/sec) than the observed mean or median regularly drove excitatory and inhibitory neuron subclasses in barrel cortex [30]. In none of these studies in reduced preparations were velocities above 2500°/sec employed. During the active sensing conditions examined here, 19% of events were above this peak velocity.

The salience of events will likely vary as a function of perceptual context [37, 38], but evidence of their relevance follows from a study in head-posted animals by Schwarz and colleagues [39]. These authors found a “low velocity” detection threshold of 125°/sec for single deflections with amplitudes larger than 3°, and a “high velocity” threshold of 750°/sec for smaller deflections (down to 1°). Relative to the present findings, even the larger velocity is below the median we observed (1125°/sec; see the red curve in Figure 5B that indicates where 3° events fall). Thus, rough surfaces, which generated high amplitude, long duration and high velocity events, should be more salient, but both rough and smooth surfaces generated events above known neural and perceptual thresholds. An important caveat to this conclusion is that there is some ambiguity in comparing estimated micro-motion parameters with stimuli of the different shapes employed across these studies (e.g. linear ramps, sinusoids, and parabolic pulses). Note also that this analysis does not account for the effect of repetitive stimuli, and in particular the sensory consequences of patterns of micro-motions across vibrissae, that are likely to be adaptive and non-linear [31, 37, 38, 40–47]. High frequency stimuli above 50 Hz, particularly those amplified by vibrissa resonance, can drive sustained activation in SI neurons [6, 18] and in the trigeminal ganglion [8, 48] in acute preparations.

DISCUSSION

The vibrissa sensory system is commonly used as a high acuity model for mammalian sensory and motor function [37, 49–52]. Despite broad interest in this system, and the consensus that vibrissa micro-motions carry relevant surface information, no prior studies have quantified these micro-motions in the awake and freely behaving animal.

The present report provides the first systematic analysis of micro-motion signals, an advance enabled by development of novel high-speed and high-resolution videographic techniques. We discovered that the mechanical embodiment of the system crucially impacts tactile inputs to the afferents, and creates significant variation across the vibrissa pad. This finding confirms predictions from previous anesthetized and *ex vivo* studies that resonance should be expressed in behaving animals during surface contact [6, 13, 18, 19], although it remains an open question if this feature was employed to enhance perception. We further determined amplitudes, velocities and rise times of micro-motions induced by contact with rough and smooth surfaces during active sensation, and found they provided substantially more robust inputs than those typically employed to probe the system.

Intrinsic Biomechanics Shape Sensory Representation by the Vibrissae

Intrinsic biomechanical properties of the vibrissae demonstrated a strong impact on tactile inputs under conditions that spanned from contact with a milled smooth surface to an aperiodic rough surface. Smaller, anterior vibrissae exhibited higher frequencies than longer, posterior vibrissae. Importantly, these variations in transduction were observed even when analysis was restricted to the highest velocity events, which are widely believed to be the most likely to induce peripheral and central neural activity [5, 9].

These findings indicate that resonance properties of the vibrissae impact the representation of sensory input, shaping those events that are likely to be most perceptually relevant. Three

central coding schemes have been suggested for the perception of surface properties (e.g. rough vs. smooth), variation in micro-motion mean frequency [18], variation in micro-motion mean velocity [7, 14] and variation in the temporal pattern of high velocity micro-motions [9]. Because intrinsic vibrissa properties play a significant role in determining micro-motion frequencies and high-velocity events, all of these schemes will be impacted by biomechanics that vary across the pad, suggesting that the initial, embodied transformations of sensory input are significant factors for currently proposed codes.

Our findings predict that central neural representations will receive a spatially organized pattern of frequency input determined by vibrissa length, an anterior-posterior ‘map’ of frequency [6]. The observation that vibrissa length predicted frequency for both rough and smooth surfaces suggests that this relation holds during a variety of active sensing contexts. If so, the structure and tuning of specific somatotopic positions within central neural representations may reflect the continued experience of this specific bandwidth of information. Further, behavioral choices during active sensing, such as whisking speed and contact distance, may be employed to take advantage of this structural feature of peripheral transduction to facilitate perception [18].

These findings are in apparent conflict with recent acute studies that did not report an influence of resonance properties on vibrissa signal transduction [9, 14]. This discrepancy could be explained by the fact that these prior studies employed small, short duration sweeps of vibrissae over a surface, using a single sweep speed, and at a single distance of the surface from the face or vibrissa base. As we describe in Figure 1, vibrissa responses will in general be a mix of surface dependent and intrinsic motions, and designating a particular motion as due to ‘resonance’ is problematic without either varying sampling conditions or using other information, e.g. spatial extent of the whisker motion. Another important potential discrepancy is that different boundary conditions at the base (e.g. due to muscle tonus or blood pressure) likely exist in behaving versus anesthetized animals (and both likely differ from *ex vivo*), which may affect the relative contributions of surface-driven and intrinsic modes [13, 18, 53]. Some previous reports that did not observe an impact of resonance have also focused their analysis exclusively on signals in a lower frequency range (e.g., <150 Hz, [14]), whereas higher frequencies were observed in the present study. As one example, the range of frequencies generated during smooth surface contact extended above 300Hz for smaller vibrissae (Figure 5). Further, high-frequency oscillations during contact can be sustained for only portions of the overall contact epoch, so Fourier methods may be misleading if the timescale of the frequency analysis is not appropriate for this class of motions.

Perhaps most importantly, prior studies on this topic relied on simulated sampling (artificial whisking), while micro-motions observed here resulted from sampling strategies chosen by behaving animals. During natural behavior, peripheral filters are often actively manipulated to optimize perception, for example saccadic and smooth pursuit eye movements that align features of interest in the visual scene with the fovea [54, 55], motion of the head and pinnae to optimize sound collection [56], context-dependent damping of cochlear transduction to maintain dynamic range [57, 58], and regulation of pressure and velocity exerted against a

surface to maintain acuity during fingertip touch [48, 59]. Our data indicate that the animal's sensing choices enabled significant biomechanical transformations of surface features.

Velocities Are Significantly Greater than Those Previously Shown to Drive Neural Activity

A significant number of the micro-motion velocities observed during active sensation substantially exceeded those typically applied during classical sensory physiology studies, suggesting that the awake behaving animal receives stronger afferent drive than is typically ascribed to this system. Moreover, a significant fraction of events exceeded the psychophysical thresholds for isolated deflections recently established in [39]. Findings from anesthetized and immobilized animals suggest that most of the micro-motions generated during active sensation are poised to drive robust neural firing in the barrel cortex, including the smaller amplitude signals generated during smooth surface contact. An even broader range of sensitivity exists in peripheral trigeminal ganglion responses [8, 48]. Important in this regard is the recent study of von Heimendahl and colleagues [16], which shows a difference in cortical multi-unit activity between rough and smooth surface contact that correlates with the animal's discrimination choice. While they did not measure micro-motions, we predict that differences during their task in line with micro-motions reported here (Figure 8) could underlie their behavioral and neural observations.

This finding indicates that current theories regarding the responsiveness of the vibrissa system may underestimate the strength of afferent drive. Specifically, several authors have suggested, based on compelling evidence across many reduced preparations where the vibrissa are manually deflected, that encoding in the vibrissa sensory system is 'sparse,' with at most a single action potential per deflection [60, 61]. The commonality of high velocity events experienced during free active sensation may drive higher firing rates than predicted by these studies, a suggestion that is supported by examples from previous studies [15, 16, 62] but awaiting systematic *in vivo* examination in single-unit recordings.

Basic Input Motifs During Active Sensation

We observed that stick-slip-ring behavior was common for interactions with a rough surface, leading to a class of large amplitude, high velocity events. The pattern of stick-slip like behavior observed during rough surface contact is consistent with previous theoretical predictions [13, 18] (see [20] for an explication of this point). Oscillatory motions were also observed during vibrissa contact with the smooth surface, but were generally smaller in amplitude and less ballistic, with a subset of vibrissae failing to demonstrate detectable micro-motions. Moreover, smooth micro-motions generally were more periodic than rough micro-motions (e.g. Figure 7). However, for both patterns of micro-motions, average micro-motion frequency depended on vibrissa length, as expected for resonance due to intrinsic mechanics. These findings highlight that resonance should not be thought of simply as the appearance of an oscillation, but is rather a "filtering" of information transduced from surface contact. Even complex, aperiodic motions, such as could be generated over our random, rough texture, are impacted by resonance by being biased towards an intrinsic frequency largely independent of surface type. This bias is thus likely to be an important component of surface discrimination on both neural and perceptual levels, although it remains open if resonance contributes positively to perception, is a "distortion" eliminated

by neural processing, or plays a more complicated role in task performance. One caveat is that the quantitative values of resonance frequencies depend on boundary conditions (e.g. muscle tonus and blood pressure in the follicle, and form of contact with the surface) [18, 29], so that the gradient of resonance frequencies from short to long vibrissae is likely a more robust phenomenon than the numerical values of the frequencies in isolation. The frequencies we found here were consistent with what we termed “fixed-free” (e.g. a plucked vibrissa in air [13, 19]) or “fixed-pinned” boundary conditions, but were approximately a factor of two smaller than what we found under “fixed-fixed” boundary conditions, as encountered with piezoelectric stimulation to the vibrissa tip [6, 13].

Differences in Interactions with Rough and Smooth Surfaces

While it was outside the scope of this study to conclusively identify the codes used by a rat during the discrimination of rough versus smooth surfaces, we discovered several differences in the pattern of events during contact with these surfaces. Our data indicated that a distinct class of large amplitude events occurs during rough surface contact. The temporal profile of these signals is also substantially different, with more periodic oscillations observed during smooth surface contact.

These data are in general in agreement with the hypothesis that the temporal pattern of high velocity micro-motions [9], either the periodicity and/or the precise timing of these events, could subserve texture discrimination. During rough surface contact, the existence of large amplitude events that had similar velocity to those during smooth contact suggests that angular deviation of the vibrissa and/or the torque applied to the base also could provide important sensory information. This suggestion is in agreement with recent studies reporting that vibrissa position is encoded in neural response properties [5, 43, 63, 64]. Similarly, recent studies have shown that measurements of the torque applied to vibrissae during object contact can lead to the accurate reconstruction of complex object features [65]. The current study does not resolve if the impact of mechanics on micro-motions we report, specifically resonance, is a necessary component of texture discrimination performance. For example, it could be that even when active sensing choices lead to resonance expression, the actual "code" used by the animal does not exploit this information, in favor of other possible decoding strategies [9, 14]. Moreover, we did not find that multiple vibrissae along a row sweep surface regions in such a way that texture information would be acquired via parallel frequency channels, a hypothesis developed from earlier reduced preparations [6, 13, 18] in analogy to the cochlear decomposition of sound waves, although we cannot rule out this possibility, e.g. for harder discriminations. The current results do show that micro-motions are strongly shaped by the intrinsic properties of the vibrissa, impacting aspects of these motions that are widely considered to be essential for driving neural activity, e.g. velocity (Figure 5). The large amplitude motions we observed during rough contact would likely generate significant neural activity, consistent with a recent report showing increased firing during rough versus smooth contact (without measuring the motions that drove this activity) [16]. Firing rate differences with different surface type have not always been observed [15]. Ultimately, the differential information provided in micro-motions during contact with different surfaces will be resolved only with simultaneous measurements of neural activity and vibrissa motion.

Conclusion and Future Studies

The present findings provide the first description of what is believed to be an essential surface cue, micro-motions of the vibrissae. In so doing, they address fundamental questions that had until this point remained unanswered, such as whether intrinsic biomechanics would impact transduction meaningfully during active sensation, and what range of velocities are produced during free behavior. We emphasize that our task did not require vibrissa contact; rats were permitted to use any strategy, including contact with other body parts or other means of discriminating surfaces. Rats chose to make contact with multiple vibrissae, and developed highly stereotyped vibrissal active sensing strategies, indicating that this system played a consistent, selected role in the task. This finding is in agreement with prior studies showing high resolution capability of vibrissae in resolving different textures and generally similar behavior patterns [10, 11, 15, 66, 67]. That said, alternative cues could have been employed. Visual input was unlikely to be a common contributor, because even under conditions of infra-red only illumination, rats performed at high accuracy (see Supplemental Data S1). Other signals, such as olfactory cues or more subtle influences of air currents surrounding the two surface types, cannot be excluded, although this task can be performed with uncued replacement of discriminanda, suggesting that rats are not simply learning the smell of previously experienced objects to guide their choices (Supplemental Data S1). Future studies designed to test this question —employing, for example, a single surface that can be manipulated in relative spacing on each trial — are required. Perhaps most importantly, studies combining high-speed imaging and simultaneous neurophysiological recordings should provide a conclusive link between the micro-motions observed and neural activation.

METHODS

We here present a brief overview of training, videographic and data analysis methods. For further details see Supplemental Data S1.

Videography: Hardware

For *ex vivo* videography, we used a MotionScope PCI 8000s (Redlake) high speed video camera. A white incandescent illuminator (Dolan Jenner) provided lighting in a pseudo-darkfield arrangement that made vibrissae appear bright on dark frames. For *in vivo* measurements we used a pco.1200hs (Cooke Corporation) high speed video camera. Illumination came from a Strobe LED (AOS), a grid of high-power infrared (~880 nm peak wavelength) LEDs pointed at a mylar diffuser placed as back-lighting, producing dark vibrissa (and head) on a bright background.

Simulated Rat: *Ex Vivo* Videography

We took plucked vibrissae from rats terminated in the course of other experiments, (Sprague Dawley, 300–500g) and drove them over surfaces with a precision motor (Maxon: Figure 1A) controlled by a variable DC power supply (Tenma 72-6628), adjusted to achieve the desired sweep speed. MotionScope acquisition was 4000 frames/sec, at either 98x100 or 68x160 pixels, with 0.321 mm per pixel resolution (e.g. Figure 1A right) or 0.056 mm per pixel resolution (e.g. Figure 5A) depending on lens choice.

Behaving Rat: Videography During Active Sensation

Long Evans rats (N = 3; weights 475g = 4B, 495g = 4R, 375g=5R at time of videography) were trained on an elevated platform to discriminate between two halves of a vertical surface with ‘rough’ and ‘smooth’ regions. Rats were trained to lick from a reward tube proximal to the S+ region for chocolate milk reward. Reward was released only after the initiation of licking, and only if licking occurred on the correct tube. Between trials, a gate placed between the rat and the surface denied access while the surface orientation was manually reset. Two red LEDs (~650nm), outside the principle visible spectrum for rats [4], provided dim illumination for the human operator, located so that no light impinged directly on the texture. Sessions with infra-red only illumination confirmed that vision was not necessary for task performance (see Figure SF1 in Supplemental Data S1, which also shows a test for object specific (e.g. olfactory) cues).

Textured surfaces were manufactured in lab from a 15 x 15 cm sheet of hard polyurethane foam with a desktop milling machine (Modela MDX-20, Roland DG). The rough region consisted of a 3 mm lattice of squares milled to random heights up to 2 mm depth, spanning 6 cm (horizontal) by 10 cm (vertical). The other half of the surface, the smooth region, was planed flat to the precision limits of the miller. The texture was located at a ~6 cm gap from the front of the platform. While restricted from climbing on the top of the surface, which untrained rats would routinely attempt, rats were not in any way constrained from sampling the surface, and they could readily reach the surface with the tip of the nose or the forepaws. Nevertheless, contact with the forepaws on the texture was never observed in a trained animal, and contact with the nose was rarely observed, including in slow video and on-line observations during performance (N = 3 rats; data not shown).

We collected video in two sessions for each of the three rats for a total of 37 trials with high speed video over all sessions. Data collection is limited by the number of minutes required to store each video from RAM to hard disk, during which the rat continued to do trials but no more video could be recorded. Technical failures prohibited analysis of video from rat 5R. After carefully reviewing the remaining videos and rejecting those with poor (untrackable) image quality, mostly due to the rat’s head not being within our narrow (~1cm) depth of focus or being only partially visible in the frame for most of the video, we retained 7 trials for intensive analysis. Viewing of all videos showed qualitative agreement with our quantitative findings. Cooke 1200hs acquisition was at 3202 frames per second, using a 50mm/f1.2 lens, for a resolution of 0.11 mm per pixel.

Data Analysis

The very high frame rates used in this study, necessary to capture fast mechanical events in the vibrissae, precluded manual vibrissa tracking and analysis. We therefore developed automated tracking software (in Matlab), as detailed in Supplemental Data S1.

Briefly, for *ex vivo* movies, we located the intersection of the vibrissa with a circle centered on the motor shaft, to get angle as a function of time, including both sweeping and micro-motions. In Figure 1D we subtracted the sweep speed to form “residual angles” (e.g. $\theta Residual(t) = \theta Measured(t) - 720*t$ for a sweep speed of 720°/sec).

For *in vivo* movies, we developed a more advanced analysis, as the vibrissae are translated due to head motion in addition to rotations due to whisking. Briefly, we manually selected the vibrissa base and orientation in an initial frame, and the tracker then iterated outward finding 4 pixel (~0.44 mm) length segments of lowest average intensity. For subsequent frames, the tracker searched for a new base location near the previous location, then repeated the process. All tracks were manually verified by playing back the video with the tracked vibrissa overlaid. We took human confirmation of tracking quality as our gold standard, since there is no unique mathematical solution.

For event analysis (Figures 7 and 8), we estimated the angle of the face at the vibrissa base, and translated and rotated the frame respectively by the base position and angle of the face to get head centered coordinates. In the absence of whisking or micro-motions, aligned movies show a stationary vibrissa across time. We converted segment positions to angles in this coordinate frame, emphasizing measurement 5 mm from the base for comparison with anesthetized studies where deflections are often initiated at this position [5, 30]. To separate whisks from micro-motions, we used a generalized additive model [68], in which the vibrissa motion was assumed to be the sum of two spline components jointly minimizing a weighted combination of fit error and smoothness. One spline was weighted towards greater smoothness (lower frequency), corresponding to whisking motions, and the other was weighted towards lower error (higher frequency), capturing micro-motions. In practice, the chosen weights corresponded to a break between whisking and micro-motion components at ~50 Hz. We then found rest crossings in the micro-motion component, and least-squares fit a 2^{nd} order polynomial between each pair of crossings to robustly estimate derivatives (see Figure 7). Micro-motion amplitudes and rise times were defined as, respectively, the maximum absolute displacement of the fit and the time from rest crossing to maximum displacement. The velocities were defined as the absolute slope of the fit at onset (the peak velocity). To compare stimulus parameters in previous studies (Figure 8B *right*), we took reported peak velocities and onset durations. Rise time was defined as the time from rest to reach maximal excursion. See Supplemental Data 1 for further details.

For *in vivo* frequency estimates (Figures 4, 5 and 6), we increased the number of vibrissae that could be measured in a given trial by setting a horizontal line immediately adjacent (~1 mm) and parallel to the surface. We then tracked vibrissa intersections with this line, to get a timeseries of vibrissa position, which we high pass filtered at 50 Hz to remove whisking and head translations, and low passed at 800 Hz to reduce high frequency noise. We found instantaneous frequencies and amplitudes at each time point via a Hilbert transform, and then averaged the instantaneous frequencies weighted by the instantaneous squared amplitudes. The amplitude squared is a measure of oscillation power, similar to the power spectral density in Fourier analysis. This method appropriately estimates frequencies of intermittent micro-motion epochs such as we observed, and rejected small amplitude high frequency noise from the estimate.

See Supplemental Data S1 for details on manual estimation of vibrissa lengths and contact probabilities, and discussion of comparison to other vibrissa tracking methods.

Supplementary Material

Refer to Web version on PubMed Central for supplementary material.

Acknowledgments

We would like to thank Howard Eichenbaum for consultation on animal training, Emery Brown and Robert Haslinger for consultation on timeseries analysis, the Edgerton Center for use of the Redlake camera and consultation on high speed videography, Amy Sun and Neil Gershenfeld at the MIT NSF Center for Bits and Atoms for consultation on precision construction of textured surfaces, and Alexis Bradshaw and Elizabeth Seivert for assistance in animal training. The work was supported by NIH RO1 NS045130 and NSF 0316933 (C. I. M.), NIH F32 NS045415 (J. T. R.) and a Howard Hughes Medical Institute predoctoral fellowship (M. A.).

References

1. von Bekesy, G. Experiments in hearing. Vol. 745. New York: McGraw Hill; 1960.
2. Geisler, C. From sound to synapse. New York: Oxford University Press; 1998.
3. Woolsey TA, Van der Loos H. The structural organization of layer IV in the somatosensory region (SI) of mouse cerebral cortex. The description of a cortical field composed of discrete cytoarchitectonic units. Brain Res. 1970; 17(2):205–42. [PubMed: 4904874]
4. Jacobs GH, Fenwick JA, Williams GA. Cone-based vision of rats for ultraviolet and visible lights. J Exp Biol. 2001; 204(Pt 14):2439–46. [PubMed: 11511659]
5. Pinto DJ, Brumberg JC, Simons DJ. Circuit dynamics and coding strategies in rodent somatosensory cortex. J Neurophysiol. 2000; 83(3):1158–66. [PubMed: 10712446]
6. Andermann ML, et al. Neural correlates of vibrissa resonance; band-pass and somatotopic representation of high-frequency stimuli. Neuron. 2004; 42(3):451–63. [PubMed: 15134641]
7. Arabzadeh E, Petersen RS, Diamond ME. Encoding of whisker vibration by rat barrel cortex neurons: implications for texture discrimination. J Neurosci. 2003; 23(27):9146–54. [PubMed: 14534248]
8. Jones LM, et al. Robust temporal coding in the trigeminal system. Science. 2004; 304(5679):1986–9. [PubMed: 15218153]
9. Arabzadeh E, Zorzin E, Diamond ME. Neuronal encoding of texture in the whisker sensory pathway. PLoS Biol. 2005; 3(1):e17. [PubMed: 15660157]
10. Carvell GE, Simons DJ. Biometric analyses of vibrissal tactile discrimination in the rat. J Neurosci. 1990; 10(8):2638–48. [PubMed: 2388081]
11. Carvell GE, Simons DJ. Task- and Subject-Related Differences in Sensorimotor Behavior during Active Touch. Somatosensory and Motor Research. 1995; 12(1):1–9. [PubMed: 7571939]
12. Guic-Robles E, Jenkins WM, Bravo H. Vibrissal roughness discrimination is barrelcortex-dependent. Behavioural Brain Research. 1992; 48:145–152. [PubMed: 1616604]
13. Neimark MA, et al. Vibrissa resonance as a transduction mechanism for tactile encoding. J Neurosci. 2003; 23(16):6499–509. [PubMed: 12878691]
14. Hipp J, et al. Texture signals in whisker vibrations. J Neurophysiol. 2006; 95(3):1792–9. [PubMed: 16338992]
15. Prigg T, et al. Texture discrimination and unit recordings in the rat whisker/barrel system. Physiol Behav. 2002; 77(4–5):671–5. [PubMed: 12527017]
16. von Heimendahl M, et al. Neuronal activity in rat barrel cortex underlying texture discrimination. PLoS Biol. 2007; 5(11):2696–2708.
17. Brecht M, Preilowski B, Merzenich MM. Functional architecture of the mystacial vibrissae. Behav Brain Res. 1997; 84(1–2):81–97. [PubMed: 9079775]
18. Moore, CI.; Andermann, ML. The vibrissa resonance hypothesis. In: Ebner, FF., editor. Neural Plasticity in Adult Somatic Sensory-Motor Systems. Taylor & Francis Publishing Group, CRC Press; 2005. p. 21-59.

19. Hartmann MJ, et al. Mechanical characteristics of rat vibrissae: resonant frequencies and damping in isolated whiskers and in the awake behaving animal. J Neurosci. 2003; 23(16):6510–9. [PubMed: 12878692]
20. Mehta S, Kleinfeld D. Frisking the whiskers: patterned sensory input in the rat vibrissa system. Neuron. 2004; 41:181–184. [PubMed: 14741099]
21. Kleinfeld D, Ahissar E, Diamond ME. Active sensation: insights from the rodent vibrissa sensorimotor system. Current Opinion in Neurobiology. 2006; 16(4):435–444. [PubMed: 16837190]
22. WI W. Analysis of Sniffing in the Albino Rat. Behavior. 1964; 12:223–244.
23. Berg RW, Kleinfeld D. Rhythmic whisking by rat: retraction as well as protraction of the vibrissae is under active muscular control. J Neurophysiol. 2003; 89(1):104–17. [PubMed: 12522163]
24. Towal RB, Hartmann MJ. Right-left asymmetries in the whisking behavior of rats anticipate head movements. J Neurosci. 2006; 26(34):8838–46. [PubMed: 16928873]
25. Mitchinson B, et al. Feedback control in active sensing: rat exploratory whisking is modulated by environmental contact. Proc Roy Soc B. 2007; 274(1613):1035–1041.
26. Bermejo R, Houben D, Zeigler HP. Optoelectronic monitoring of individual whisker movements in rats. J Neurosci Methods. 1998; 83(2):89–96. [PubMed: 9765121]
27. Knutsen PM, Pietr M, Ahissar E. Haptic object localization in the vibrissal system: behavior and performance. J Neurosci. 2006; 26(33):8451–64. [PubMed: 16914670]
28. Hartmann MJ. Active sensing capabilities of the rat whisker system. Auton Robots. 2001; 11:249–254.
29. Volterra, E. Dynamics of Vibrations. Columbus: Charles E. Merrill Books, Inc; 1965. p. 610
30. Andermann ML, Moore CI. A somatotopic map of vibrissa motion direction within a barrel column. Nat Neurosci. 2006; 9(4):543–51. [PubMed: 16547511]
31. Hartings JA, Simons DJ. Thalamic relay of afferent responses to 1- to 12-Hz whisker stimulation in the rat. J Neurophysiol. 1998; 80(2):1016–9. [PubMed: 9705491]
32. Shoykhet M, Doherty D, Simons DJ. Coding of deflection velocity and amplitude by whisker primary afferent neurons: implications for higher level processing. Somatosens Mot Res. 2000; 17(2):171–80. [PubMed: 10895887]
33. Temereanca S, Simons DJ. Local field potentials and the encoding of whisker deflections by population firing synchrony in thalamic barreloids. J Neurophysiol. 2003; 89(4):2137–45. [PubMed: 12612019]
34. Deschenes M, Timofeeva E, Lavallee P. The relay of high-frequency sensory signals in the Whisker-to-barreloid pathway. J Neurosci. 2003; 23(17):6778–87. [PubMed: 12890771]
35. Wilent WB, Contreras D. Synaptic responses to whisker deflections in rat barrel cortex as a function of cortical layer and stimulus intensity. J Neurosci. 2004; 24(16):3985–98. [PubMed: 15102914]
36. Wilent WB, Contreras D. Dynamics of excitation and inhibition underlying stimulus selectivity in rat somatosensory cortex. Nat Neurosci. 2005; 8(10):1364–70. [PubMed: 16158064]
37. Moore CI, Nelson SB, Sur M. Dynamics of neuronal processing in rat somatosensory cortex. Trends Neurosci. 1999; 22(11):513–20. 1_00001452–1_00001452. [PubMed: 10529819]
38. Moore CI. Frequency-dependent processing in the vibrissa sensory system. J Neurophysiol. 2004; 91(6):2390–9. [PubMed: 15136599]
39. Stuttgen MC, Ruter J, Schwarz C. Two psychophysical channels of whisker deflection align with two neuronal classes of primary afferents. Journal of Neuroscience. 2006; 26(30):7933–7941. [PubMed: 16870738]
40. Garabedian CE, et al. Band-pass response properties of rat SI neurons. J Neurophysiol. 2003
41. Sheth BR, Moore CI, Sur M. Temporal modulation of spatial borders in rat barrel cortex. J Neurophysiol. 1998; 79(1):464–70. [PubMed: 9425214]
42. Simons DJ. Response properties of vibrissa units in rat SI somatosensory neocortex. J Neurophysiol. 1978; 41(3):798–820. [PubMed: 660231]
43. Simons DJ, Carvell GE. Thalamocortical response transformation in the rat vibrissa/barrel system. J Neurophysiol. 1989; 61(2):311–30. [PubMed: 2918357]

44. Shimegi S, et al. Physiological and anatomical organization of multiwhisker response interactions in the barrel cortex of rats. J Neurosci. 2000; 20(16):6241–8. [PubMed: 10934274]
45. Benison AM, et al. Temporal Patterns of Field Potentials in Vibrissa/Barrel Cortex Reveal Stimulus Orientation and Shape. J Neurophysiol. 2006
46. Barth DS. Submillisecond synchronization of fast electrical oscillations in neocortex. J Neurosci. 2003; 23(6):2502–10. [PubMed: 12657711]
47. Castro-Alamancos MA, Oldford E. Cortical sensory suppression during arousal is due to the activity-dependent depression of thalamocortical synapses. J Physiol. 2002; 541(Pt 1):319–31. [PubMed: 12015438]
48. Gibson JM, Welker WI. Quantitative studies of stimulus coding in first-order vibrissa afferents of rats. 2. Adaptation and coding of stimulus parameters. Somatosens Res. 1983; 1(2):95–117. [PubMed: 6679920]
49. Simons, DJ. Neuronal Integration in the somatosensory whisker/barrel cortex. In: Jones, EG.; Irving, T., editors. Cerebral Cortex. Vol. 11. New York: Plenum Press; 1995.
50. Keller, A. Synaptic Organization of barrel cortex. In: Jones, EG.; Diamond, IT., editors. Cerebral Cortex. Plenum Press; New York, NY: 1995. p. 221-262.
51. Kleinfeld D, et al. Adaptive filtering of vibrissa input in motor cortex of rat. Neuron. 2002; 34(6): 1021–34. [PubMed: 12086648]
52. Nishimura N, et al. Targeted insult to subsurface cortical blood vessels using ultrashort laser pulses: three models of stroke. Nat Methods. 2006; 3(2):99–108. [PubMed: 16432519]
53. Yohro T. Structure of the sinus hair follicle in the big-clawed shrew, Sorex unguiculatus. J Morphol. 1977; 153(2):333–53. [PubMed: 894728]
54. Reinagel P, Zador AM. Natural Scene Statistics at the Centre of Gaze. Network: Computation in Neural Systems. 1999; 10:341–350.
55. Einhauser W, et al. Human head-eye co-ordination in naural exploration. Network. 2007; 18(3): 267–297. [PubMed: 17926195]
56. Easton RD. The effect of head movements on visual and auditory dominance. Perception. 1983; 12(1):63–70. [PubMed: 6646955]
57. Suga N, et al. The corticofugal system for hearing: recent progress. Proc Natl Acad Sci U S A. 2000; 97(22):11807–14. [PubMed: 11050213]
58. Maison S, Micheyl C, Collet L. Influence of focused auditory attention on cochlear activity in humans. Psychophysiology. 2001; 38(1):35–40. [PubMed: 11321619]
59. Smith AM, Scott SH. Subjective scaling of smooth surface friction. J Neurophysiol. 1996; 75(5): 1957–62. [PubMed: 8734594]
60. Kerr JND, et al. Spatial organization of neuronal populations in layer 2/3 of rat barrel cortex. Journal of Neuroscience. 2007; 27(48):13316–13328. [PubMed: 18045926]
61. Margrie TW, Brecht M, Sakmann B. In vivo, low-resistance, whole-cell recordings from neurons in the anaesthetized and awake mammalian brain. Pflugers Arch. 2002; 444(4):491–8. [PubMed: 12136268]
62. Krupa DJ, et al. Layer-specific somatosensory cortical activation during active tactile discrimination. Science. 2004; 304(5679):1989–92. [PubMed: 15218154]
63. Szwed M, Bagdasarian K, Ahissar E. Encoding of vibrissal active touch. Neuron. 2003; 40(3):621–30. [PubMed: 14642284]
64. Mehta SB, et al. Active spatial perception in the vibrissa scanning sensorimotor system. PLoS Biol. 2007; 5(2):e15. [PubMed: 17227143]
65. Solomon JH, Hartmann MJ. Biomechanics: robotic whiskers used to sense features. Nature. 2006; 443(7111):525. [PubMed: 17024083]
66. Harvey MA, Bermejo R, Zeigler HP. Discriminative whisking in the head-fixed rat: optoelectronic monitoring during tactile detection and discrimination tasks. Somatosens Mot Res. 2001; 18(3): 211–22. [PubMed: 11562084]
67. Guic-Robles E, Valdivieso C, Guajardo G. Rats can learn a roughness discrimination using only their vibrissal system. Behavioural Brain Research. 1989; 31:285–289. [PubMed: 2914080]

68. Hastie, TTR.; Friedman, J. Springer Series in Statistics. New York: Springer-Verlag; 2001. The Elements of Statistical Learning; p. 508

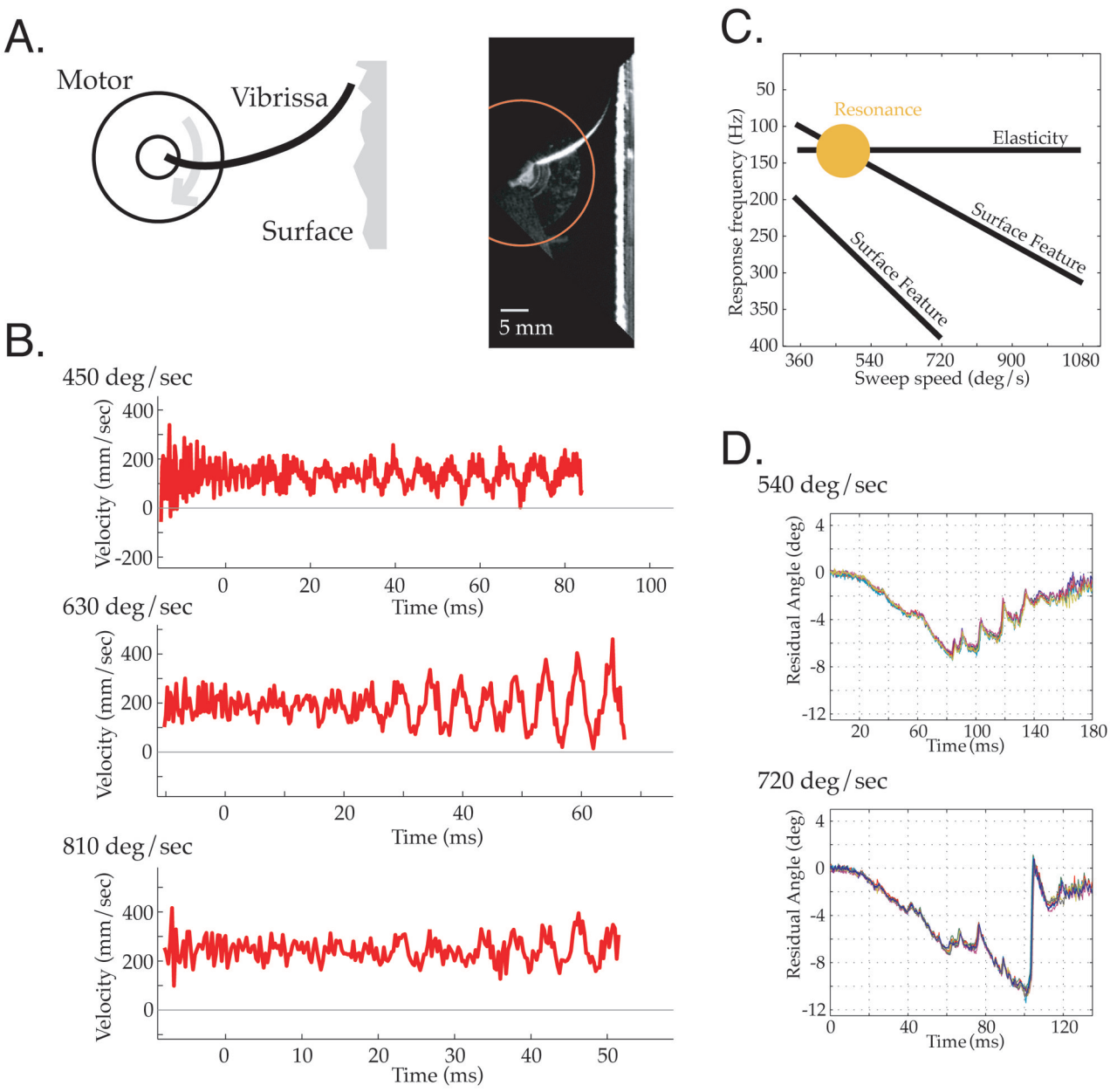

Figure 1. ***Ex vivo*** **Vibrissa Micro-Motions**

A. (left) A torque motor was used to sweep vibrissae at realistic 'whisk' speeds across sensory surfaces. (right) Still frame of a vibrissa contacting sandpaper. Angular position was measured by the intersection of vibrissae with the red circle. B. The average of 6 vibrissa micro-motion traces shown for three sweep speeds over a periodic grating. Movement of the vibrissae at an intermediate sweep speed, 630°/sec, recruited larger amplitude oscillations than movement at slower or higher sweep speeds. This selective amplification indicates vibrissa resonance tuning, and highlights the impact that variations in sweep speed can have on the form of micro-motions generated by surface contact. C. Schematic of predicted dependence between intrinsic elastic properties of the vibrissa (fundamental resonance

frequency, horizontal line) and the sweep speed of vibrissa motion (x axis) across frequency (y axis). Sweeping the vibrissa across a texture with given spatial frequencies will induce temporal responses (diagonal lines), with amplification (filled disk) at an appropriate sweep speed. D. Micro-motions from a vibrissa swept at two different velocities over sandpaper, with a fixed distance of 24.5mm from the base (vibrissa length 32mm). Each panel shows 8 repeated measurements of the same sweep conditions. The time bases are scaled in the ratio 540/720, to align micro-motions generated by the same surface features. Vibrissae generated micro-motion patterns with high consistency across sweeps, but micro-motion patterns changed substantially with a change in sweep speed.

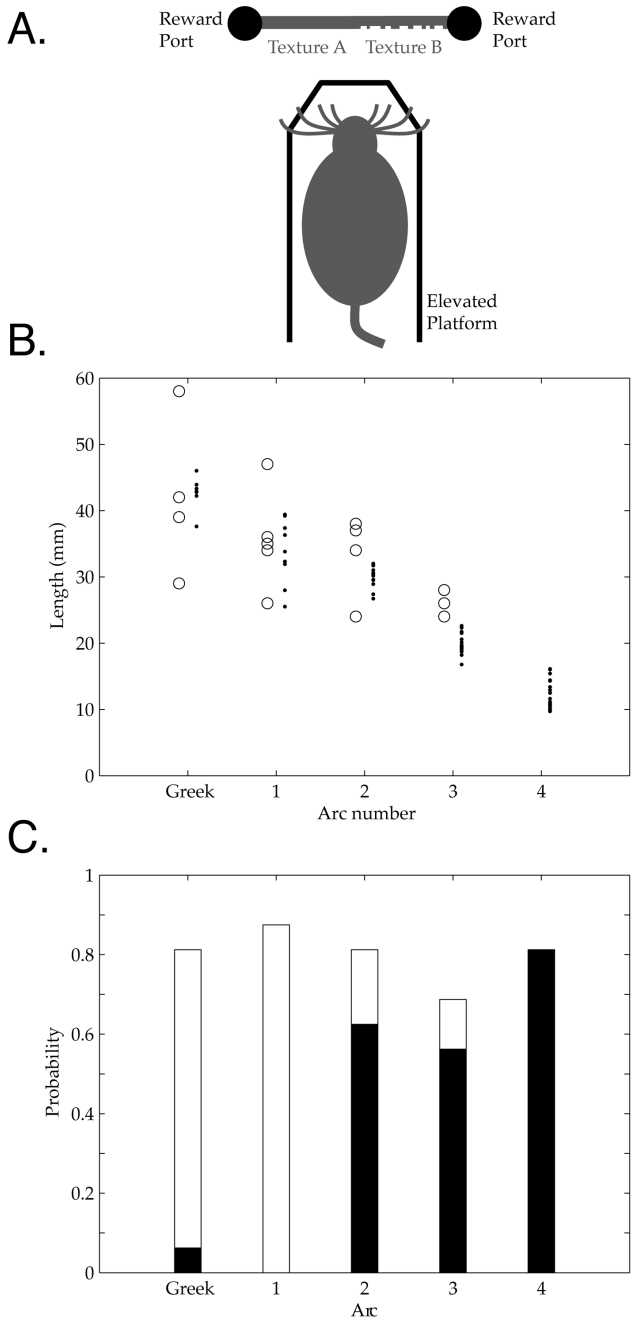

Figure 2. Stereotypy of vibrissa structure and sampling behaviors during the task

A. Schematic of behavior apparatus B. Vibrissa lengths by arc in A to D rows, estimated from high speed videos (N=4) from one session with Rat 4B (dots, one for each video and vibrissa), and comparison to *ex vivo* lengths from Table 2 of [13] (circles), showing consistent gradient of length with arc position. C. Probabilities that a vibrissa in a given arc did (black) or did not (white) make contact with the surface during the same trials. Total probability is below one due to vibrissae whose contact category could not be conclusively

determined from the video. At least one vibrissa in each of the 2, 3 and 4 arcs made contact in every trial (not shown).

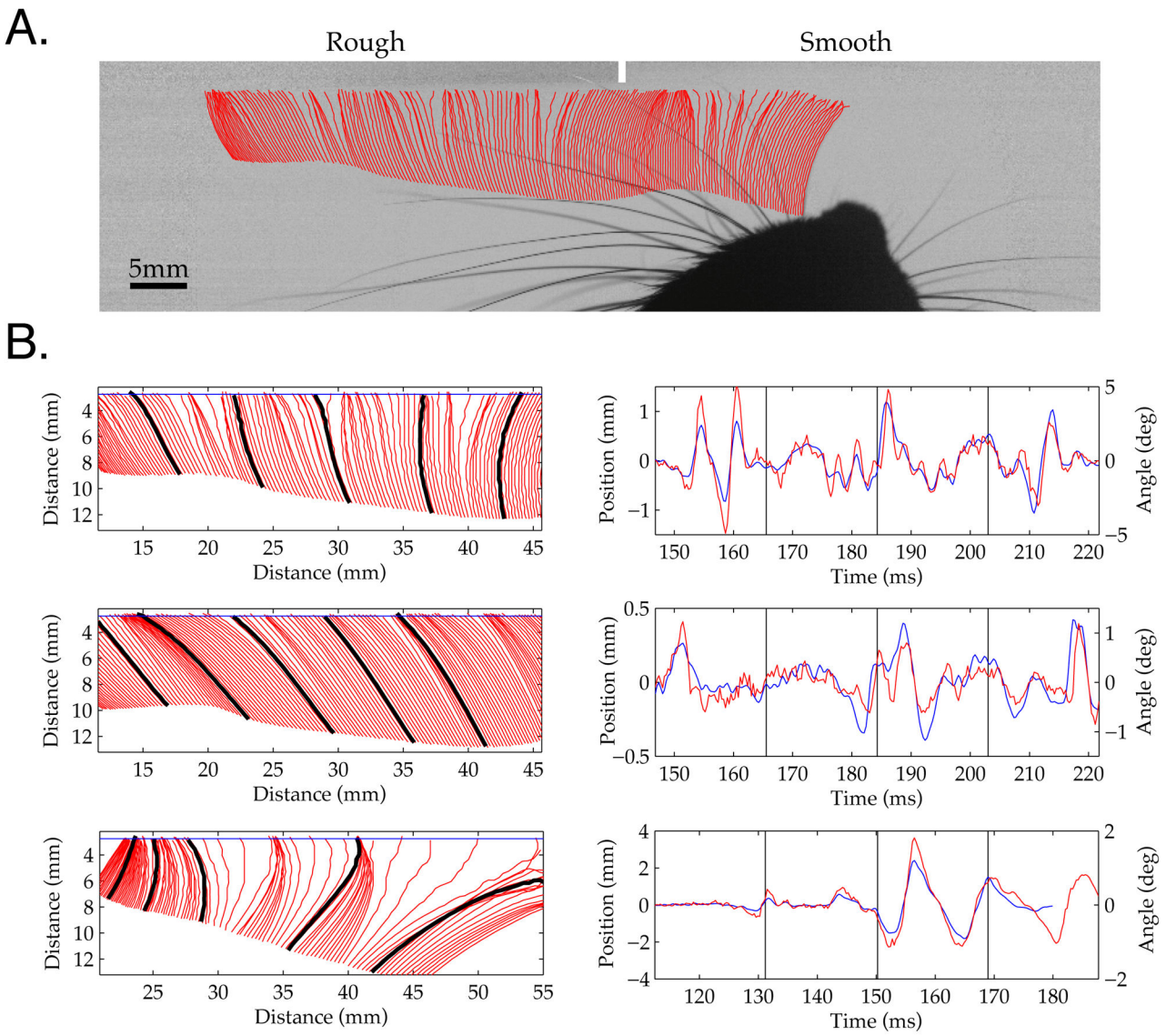

Figure 3. Vibrissa Micro-Motions During Active Sensing of a Rough Surface

A. Single frame from high speed video while a rat swept its vibrissae laterally across the surface. The red lines show the tracked positions of an anterior vibrissa every 3rd frame (~1 msec period) prior to the underlying frame. Regions where tracks are more densely spaced indicate slower motion (sticking). The small white vertical bar demarcates the border between the rough and smooth surfaces, which were removed by intensity normalization. This example is taken from a Supplemental Movie S2. B. Three examples of vibrissae tracked during simultaneous contact with the rough surface from the same trial as Figure 3A. The panel on the left shows every 3rd vibrissa track in a region of surface interaction (zero distance is the top left corner of the frame). On the right, the red timeseries is the face-centered angle of motion 5 mm from the face, and the blue line is the simultaneous vibrissa motion through a 'line scan' placed ~1 mm from the surface (see **Methods**; horizontal blue line at left). Time zero is arbitrarily chosen just before any vibrissa made surface contact.

Black lines on the tracks on the left indicate the vertical divisions in the timeseries on the right (leftmost black mark indicates the onset of the timeseries). The top two vibrissae were from the left side of the face, the bottom vibrissa from the right. As was typical of rough surface interactions, all three vibrissae demonstrated stick-slip behavior, where the vibrissa decelerated for a sustained period, built tension, and then moved rapidly forward in a ballistic manner, until again decelerating. In many cases, this sudden deceleration following a slip was followed by ringing of the vibrissa, a period of high frequency oscillations (for example, three cycles within 185 to 195 msec in B (top); note the ringing is more pronounced at 5 mm (red) than near the contact point (blue)).

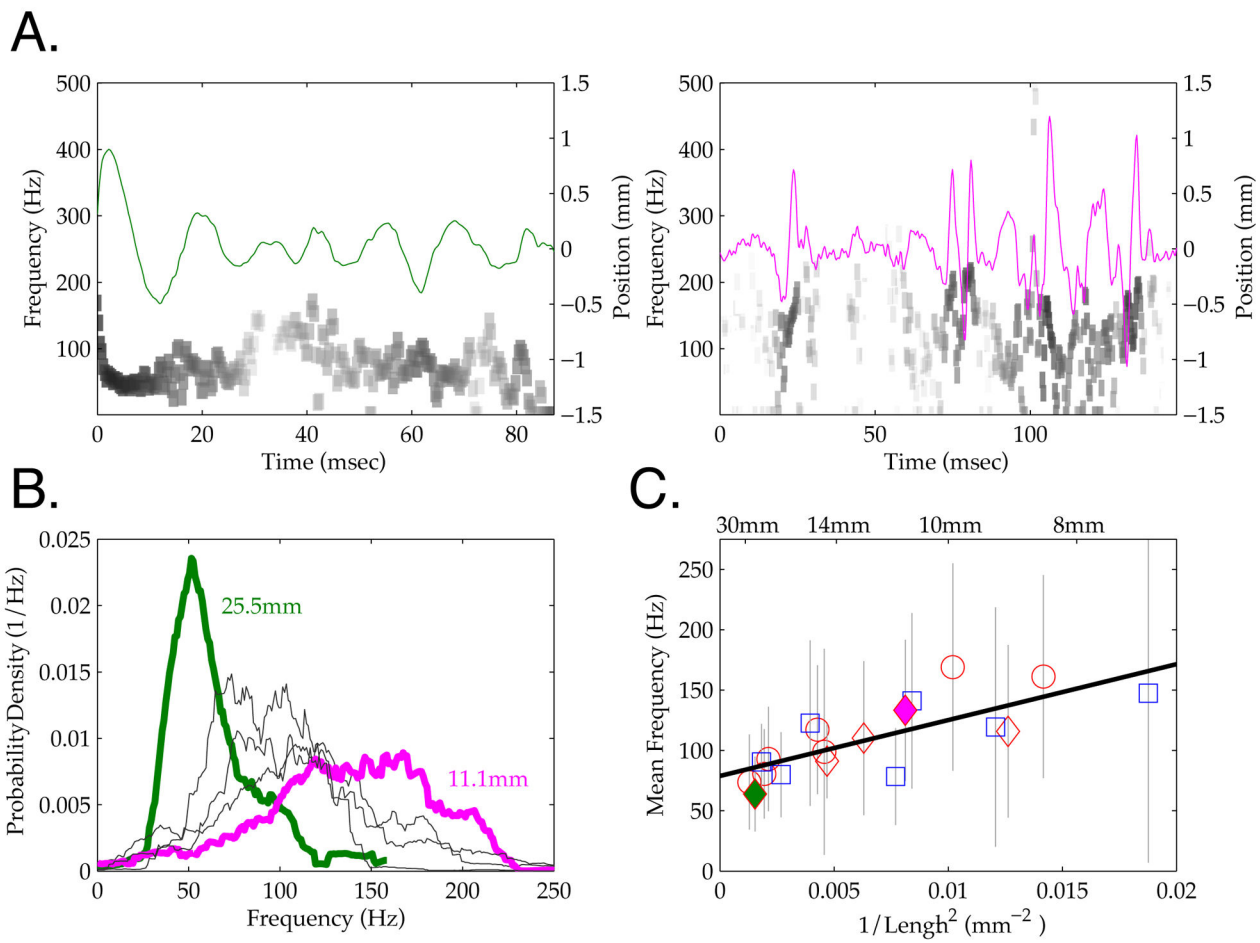

Figure 4. Vibrissa Frequency Gradient During Rough Surface Contact

A. Micro-motion timeseries are shown for two vibrissae during simultaneous contact with a rough surface (green and magenta lines, axis on right). Grayscale shows the instantaneous power (log scale) measured across frequency and time by a Hilbert transform (axis on left: see **Methods**). Distinct differences in frequency can be observed for the two vibrissae, reflecting the frequency difference evident in the motion trace. Note differences in time scale (x axis). B. The distribution of micro-motion frequencies for 5 vibrissae that contacted a rough surface during the same trial. The distribution from the line scan in the left hand panel of 4A is shown in green, and that from the right hand shown in magenta; annotation provide the lengths of these vibrissa. C. The mean frequency (symbols) and standard deviations (grey bars) for all scanned vibrissae (N = 19) during rough surface contact is plotted against 1/Length^2. Red and blue color indicate data from two rats, common symbols indicate samples from distinct vibrissae on the same trial. As described in the text, a significant linear relationship was observed between length and frequency (black line), as predicted by the mechanical properties of the vibrissae. Note that this relation held not only for the population measured across multiple trials, but also for simultaneous contact of multiple vibrissae within each trial.

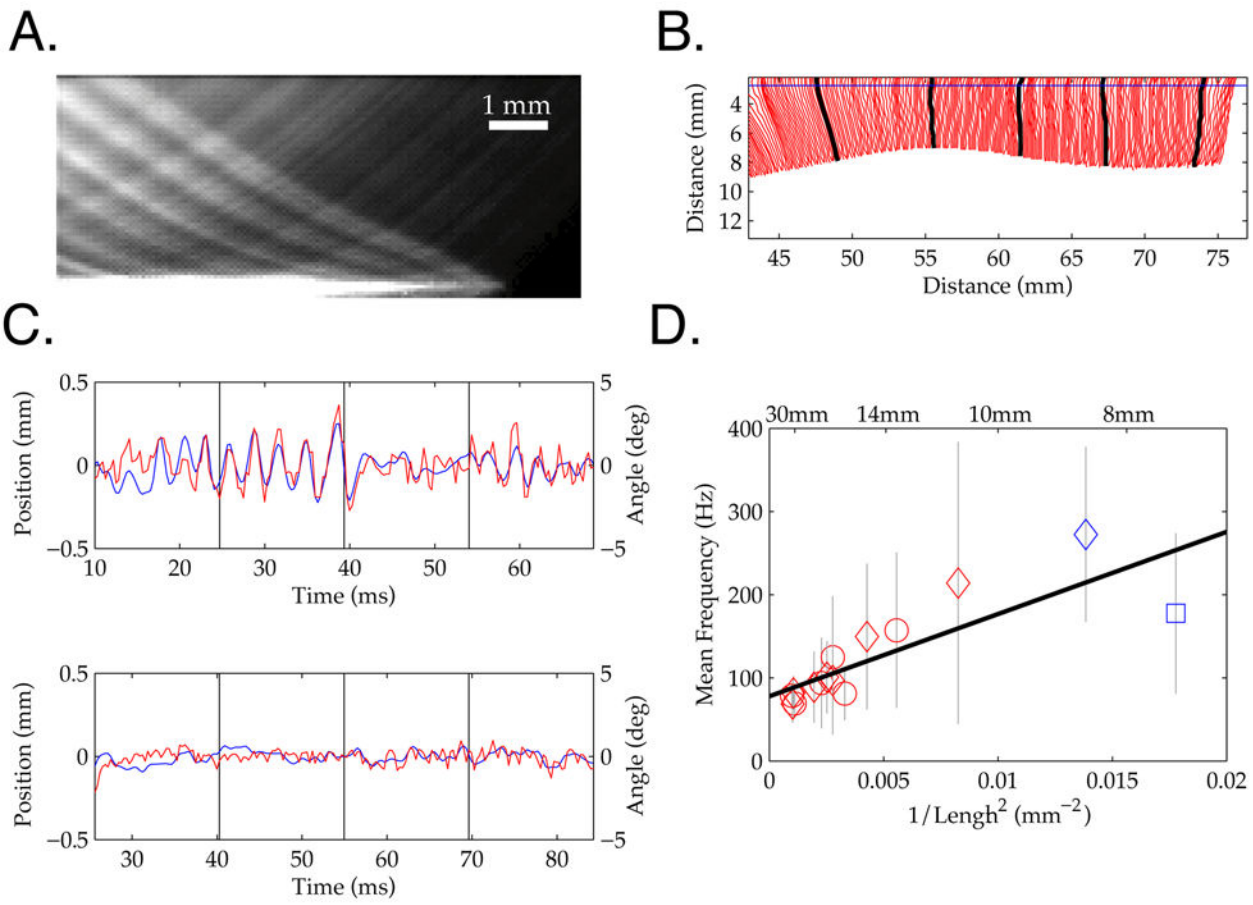

Figure 5. Vibrissa Contact with a Smooth Surface

A. Average intensity across all frames in a movie of an *ex vivo* vibrissa sweeping across glass (see **Methods** and Figure 1). Lighter regions of the image indicate positions of lower vibrissa velocity. An oscillatory pattern can be seen even though the vibrissa is not being obstructed by macroscopic features, suggesting the importance of frictional interactions. B. A track from an *in vivo* vibrissa during active surface contact with the smooth surface, every frame is shown (~0.3 msec period). Line-marking conventions as in Figure 3. C. Two tracks and line scans from vibrissae simultaneously contacting a smooth surface within a trial. These data correspond to Supplemental Movie S3. The data show that while robust oscillatory behavior was observed in one of the vibrissae during smooth surface contact, no detectable signal was present on a neighboring vibrissa, indicating the diversity of surface interactions. D. The mean frequency and standard deviations for all scanned vibrissae that showed significant micro-motions (N = 15) during smooth surface contact is plotted against 1/Length^2. See Figure 4 for legend descriptions.

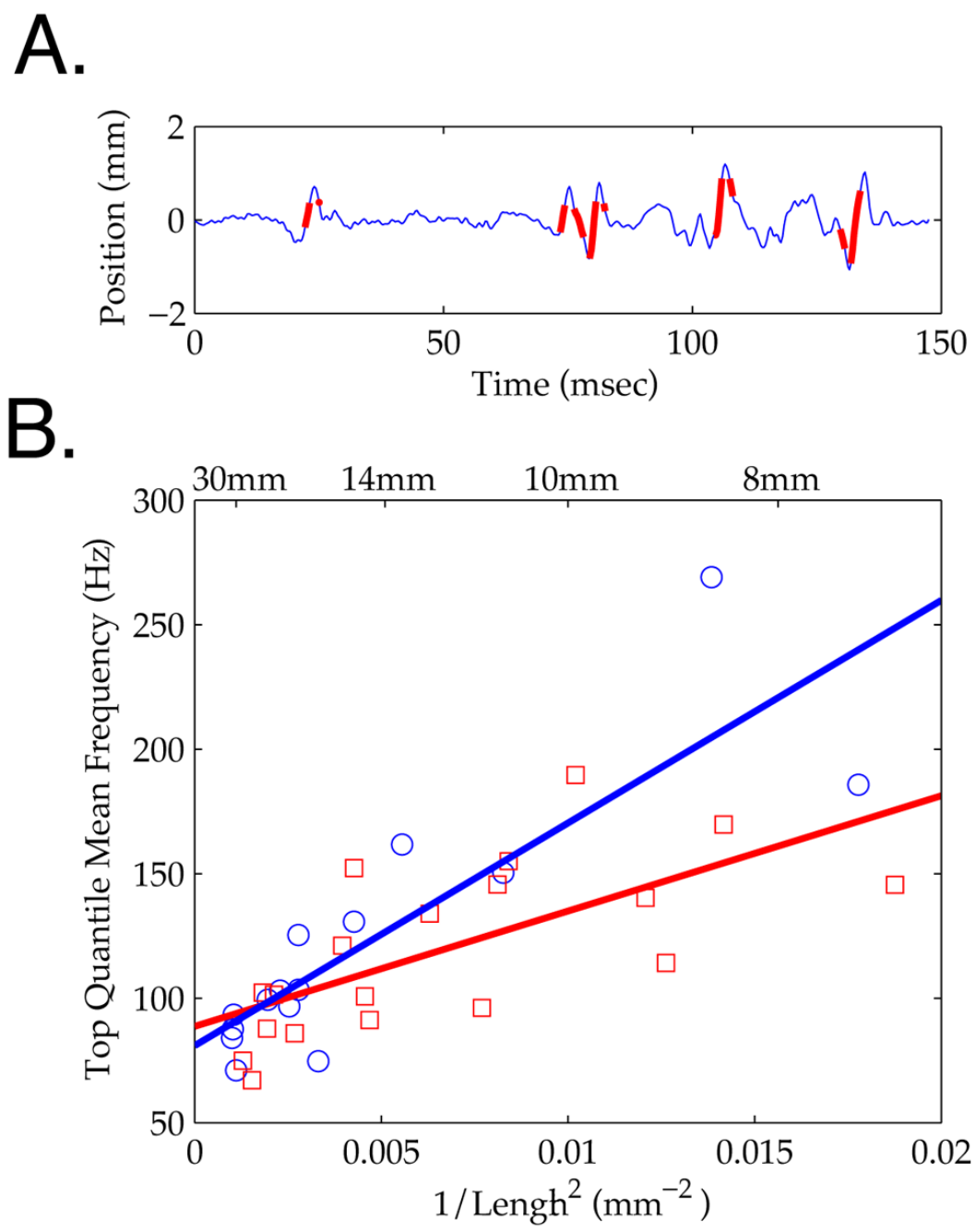

Figure 6. Frequency Gradient with Length for Highest Velocity Micro-Motions

A. Example vibrissa micro-motion trace (blue), with time points in the highest 10% of velocity overlaid (thick red). B. Mean Hilbert frequency for high velocity time points plotted against 1/Length^2, showing the same linear relationship as in Figures 4 and 5. Symbol type indicates rough (red square) or smooth (blue circle) contact; lines are corresponding linear regressions (see text).

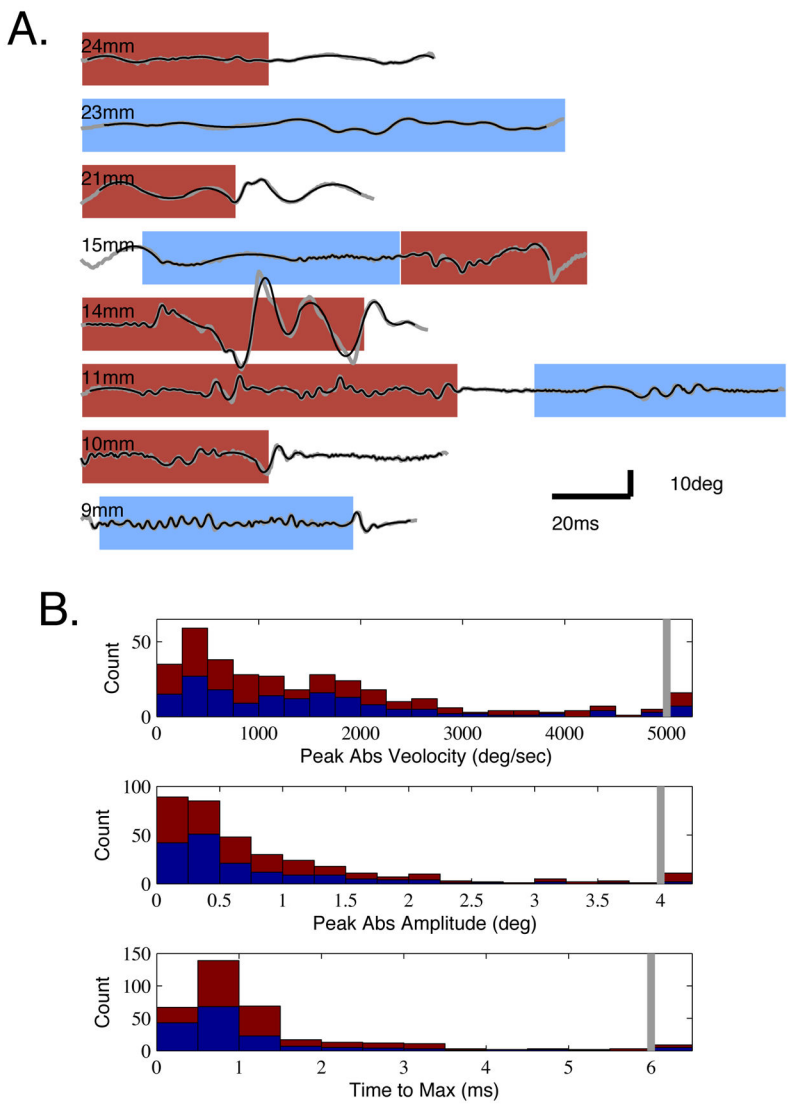

Figure 7. Examples of Micro-Motion Patterns and Marginal Distributions of Event Parameters During Contact with Rough and Smooth Surfaces

A. Example timeseries (gray) of angular position measured 5mm from the base in head centered coordinates. Traces are ordered from long to short vibrissa (top to bottom), with lengths indicated by the legends. The 2nd order fits used to define event parameters are overlaid (black). Times of rough (red) and smooth (blue) surface contact are indicated by shaded backgrounds. B. Histograms of three micro-motion parameters: peak velocity, amplitude and rise time. Red indicates events occurring during rough surface contact, and blue indicates smooth surface contact, stacked together. All observations in the bin to the right of the gray bars are totals for events greater than that value (e.g., greater than 5000°/sec velocity in the top plot).

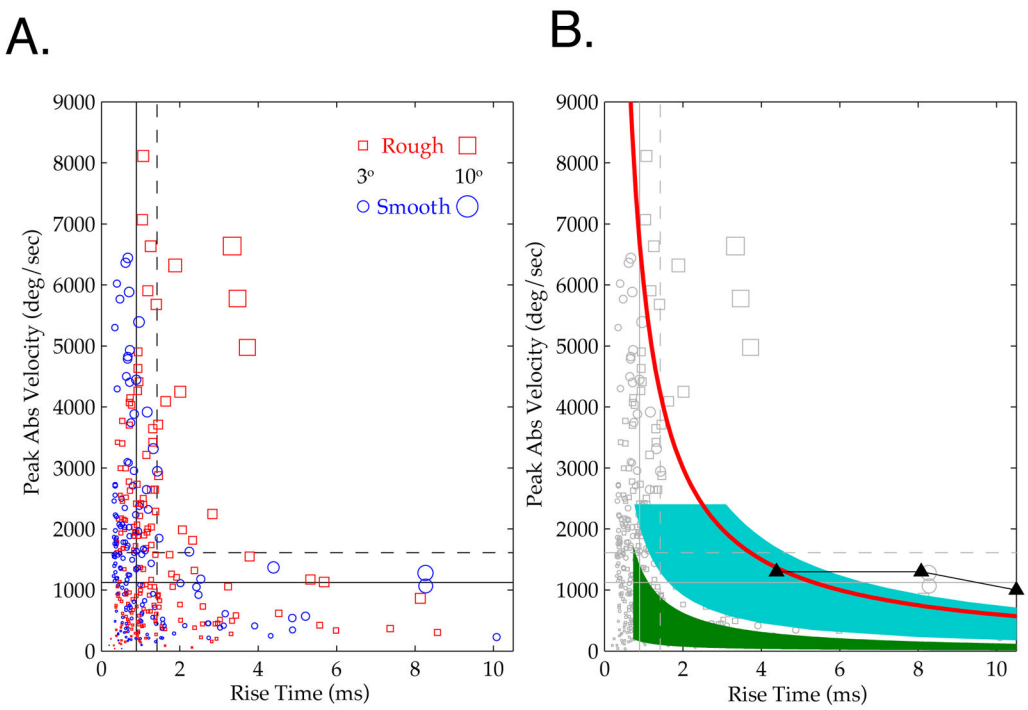

Figure 8. Joint Distribution of Micro-Motion 'Events' During Contact with Rough and Smooth Surfaces

A. Scatterplot showing the joint peak velocity and rise time distribution of all events. Color and shape indicates rough (red squares) and smooth (blue circles) contact events. Size of shape indicates the amplitude of the event, as shown in the figure legend. Dashed lines demarcate the means across all events, and solid lines demarcate the medians. A distinct class of high amplitude events occurs for rough contact. B. Same scatterplot data (grey) with overlaid patches representing stimulus parameters from previous studies that conducted parametric analyses of neuronal responses (blue [5, 31–33], green [7], black curve with triangles [35, 36]). The red curve demarcates events of 3° amplitude, separating high velocity and low velocity psychophysical "channels" found in head posted rats [39]. See text and **Methods** for details.